

OAK RIDGE NATIONAL LABORATORY

MANAGED BY UT-BATTELLE FOR THE DEPARTMENT OF ENERGY

Gary L. Bell, Ph.D.
Fusion Energy Division
P.O. Box 2008, Bldg. 4508, Rm. 271
Oak Ridge, TN 37831-6092
(865) 241-4400
E-Mail: bellgl@ornl.gov

September 24, 2004

AGR-1016

Dr. Madeline A. Feltus
Manager, Advanced Gas Reactor
NE-20, Building GTN
Department of Energy
1000 Independence Avenue, SW
Washington, DC 20585-1290

Dear Dr. Feltus:

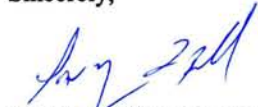
DE-AC05-00OR22725, Transmittal of Central File – ORNL/CF-04/12, “Data Summary for Nominal 350 μm DUO₂ Kernels”

Reference 1. Letter to M. A. Feltus, “DE-AC05-00OR22725, Milestone Completion, “AGR Task 3.1.2 Complete Fabrication of 3.5kg of Nominal 350 μm Diameter Depleted UO₂ Kernels,” March 29, 2004.

The purpose of this letter is to provide you with a copy of the data summary report ORNL/CF-04/12 that documents the results of the ORNL activity to characterize 350 μm diameter depleted uranium UO₂ kernels fabricated for the AGR Program by ORNL under Task 3.1.2 Kernel Manufacture (Reference 1). The central file document is not a program deliverable but does provide a record of the work performed and is given to you and program participants for information purposes.

If you have any questions, please contact me at 865-241-4400 or John Hunn at 865-574-2480.

Sincerely,



Gary L. Bell, Manager
Advanced Gas Reactor Program

GLB:jzp

Attachment

cc: E. E. Bloom
S. R. Greene

S. R. Martin, Jr. (DOE-ORO)
S. L. Milora

c/att: J. D. Hunn
R. E. Korenke (INEEL)
R. A. Lowden
R. N. Morris
P. J. Pappano

D. A. Petti (INEEL)
J. J. Saurwein (GA)
D. F. Williams
S. J. Zinkle
File-RC

OAK RIDGE
NATIONAL LABORATORY

MANAGED BY UT-BATTELLE
FOR THE DEPARTMENT OF ENERGY



ORNL-27 (4-00)

DOCUMENT AVAILABILITY

Reports produced after January 1, 1996, are generally available free via the U.S. Department of Energy (DOE) Information Bridge.

Web site <http://www.osti.gov/bridge>

Reports produced before January 1, 1996, may be purchased by members of the public from the following source.

National Technical Information Service
5285 Port Royal Road
Springfield, VA 22161
Telephone 703-605-6000 (1-800-553-6847)
TDD 703-487-4639
Fax 703-605-6900
E-mail info@ntis.fedworld.gov
Web site <http://www.ntis.gov/support/ordernowabout.htm>

Reports are available to DOE employees, DOE contractors, Energy Technology Data Exchange (ETDE) representatives, and International Nuclear Information System (INIS) representatives from the following source.

Office of Scientific and Technical Information
P.O. Box 62
Oak Ridge, TN 37831
Telephone 865-576-8401
Fax 865-576-5728
E-mail reports@adonis.osti.gov
Web site <http://www.osti.gov/contact.html>

This report was prepared as an account of work sponsored by an agency of the United States Government. Neither the United States Government nor any agency thereof, nor any of their employees, makes any warranty, express or implied, or assumes any legal liability or responsibility for the accuracy, completeness, or usefulness of any information, apparatus, product, or process disclosed, or represents that its use would not infringe privately owned rights. Reference herein to any specific commercial product, process, or service by trade name, trademark, manufacturer, or otherwise, does not necessarily constitute or imply its endorsement, recommendation, or favoring by the United States Government or any agency thereof. The views and opinions of authors expressed herein do not necessarily state or reflect those of the United States Government or any agency thereof.

Data Summary for Nominal 350 μm DUO₂ Kernels

J.D. Hunn and A.K. Kercher, Oak Ridge National Laboratory

1 Scope of report:

This document is a compilation of characterization data obtained on the nominal 350 μm depleted uranium oxide kernels (DUO₂) produced by ORNL for the Advanced Gas Reactor Fuel Development and Qualification Program under task 3.1.2. Samples were riffled for analysis from a 100 g batch (designated as DUN350-1), which was riffled from the 3.4 kg composite lot of DUO₂ kernels (designated as DUN350).

2 Summary of results:

Table 2-1 contains a summary of property measurements in comparison to the current acceptance criteria for depleted 350 μm UO₂ kernels. All the criteria were met with the exception of the 95% confidence criteria on the impurity levels, which was only measured on a single small sample. In addition, microstructure was analyzed by scanning electron microscopy (SEM). The grain size was less than 10 μm across in the plane of the cross section and typically about 5 μm . SEM micrographs also provided evidence of closed pores that were less than 0.25 μm in diameter.

Table 2-1: Summary of property measurements compared to current acceptance criteria.

Property	Specification {variable or attribute}	Value
Means of individual impurities [ppm-wt] Li, Na, Ca, V, Cr, Mn, Fe, Co, Ni, Cu, Zn, Al, Cl	≤ 100 each at 95% confidence level {variable}	see section 5 ^a
Mean bulk density [Mg/m^3] (95% confidence interval)	≥ 10.5 at 95% confidence level {variable}	10.87 – 10.97
Mean diameter [μm] (95% confidence interval)	350 ± 10 at 95% confidence level {variable}	353 – 355
Diameter [μm] (upper and lower limits to a 95% confidence level)	$\leq 1\%$ beyond each critical limit (to 95% confidence level): upper limit 400 lower limit 300 {variable}	$\leq 1\%$ beyond each limit given below (to 95% confidence level): upper limit 365 lower limit 344
Sphericity ($D_{\text{max}}/D_{\text{min}}$) (% above control limit at a 95% confidence level)	Tolerance limit $\leq 1\%$ allowed with sphericity above 1.05 control limit (to 95% confidence level) {attribute}	Based on measured sample, $\leq 0.4\%$ with sphericity above 1.05 (to 95% confidence level)

^a Confidence level was not determined, because impurity content was only measured on a single small sample. A 95% confidence level is not necessary for the current stage of research.

3 Size and shape measurement: (Kercher, Hunn, Price)

Size and shape were measured by shadow imaging a sample of kernels in a random plane with an optical microscope. Image analysis software was used to find the center of each kernel and identify 360 points around the perimeter. Data was extracted as both radius and diameter. Since the kernels were not perfect spheres, the terms “radius” and “diameter” are used loosely. “Radius” means the distance from the fit center to the edge. “Diameter” means the distance from edge to edge in a line passing through the fit center. Data for each kernel was then reported in terms of the mean radius or diameter, the standard deviation in those values, the minimum and maximum radius or diameter, and the ratio of the maximum over the minimum of those values (the aspect ratio). These values for each kernel were then compiled and the average, standard deviation, minimum, and maximum for each value were calculated. In addition to reporting the compiled data for the sample, histograms of the mean kernel radius or diameter and the aspect ratios have also been provided to show how these values were distributed in the sample analyzed.

3.1 *First analysis of DUN350 – low magnification*

Figure 3-1 shows the summary data for the measured radius of 8630 kernel shadowgraphs. Figure 3-2 shows the same data reported in terms of the diameter. The difference between compiling the measurements in terms of radius versus diameter is that the radius-based measurements more accurately report asymmetric shapes. The diameter measurements dilute the effect of a local deviation in radius by adding the opposite radius (+180 degrees in polar coordinates). Because the kernels were nearly spherical, there was no significant difference in the statistically calculated mean diameter from twice the mean radius. Even the standard deviations in these values scale by a factor of two. However, the max/min aspect ratio was significantly affected, because aspect ratios are based on maximum and minimums as opposed to means. R_{\max}/R_{\min} is a more sensitive way of measuring the deviation from a circular cross section. The R_{\max}/R_{\min} measurement showed a higher average aspect ratio as well as a broader distribution toward higher values. To be consistent with historical techniques and reports, radius-based and diameter-based aspect ratios will be herein called “sphericities,” although sphericity has several more commonly used definitions.

One effect that must be accounted for in the aspect ratio measurement of sphericity is the effect of the measurement uncertainty for ratios of this type, which are based on selecting maximum and minimum values. When a single maximum is selected, the random fluctuation from the measurement uncertainty becomes a positive bias. A similar negative bias is introduced in selecting the minimum value. This leads to a positive offset in the aspect ratio. Eq. 3.1 derives the offset ($+2\Delta R/R_{\text{mean}}$) created in the radius-based aspect ratio due to this positive and negative bias, where the bias is estimated as ΔR . The uncertainty in determining the kernel edge is usually equivalent to about 1 pixel size. For the magnification used in Figure 3-1, the pixel size was 0.895 microns. The bias ΔR can usually be estimated to be close to this measurement uncertainty. A similar offset can be derived for diameter-based sphericity with ΔD equivalent to about 2 pixel sizes (one pixel for each edge), but the offset simplifies to the same expression, $+2\Delta D/D_{\text{mean}}$.

Eq. 3.1

$$\frac{R_{\max} + \Delta R}{R_{\min} - \Delta R} = \frac{\frac{R_{\max}}{R_{\min}} + \frac{\Delta R}{R_{\min}}}{1 - \frac{\Delta R}{R_{\min}}} = \left(\frac{R_{\max}}{R_{\min}} + \frac{\Delta R}{R_{\min}} \right) \left(1 + \frac{\Delta R}{R_{\min}} + \left(\frac{\Delta R}{R_{\min}} \right)^2 + \dots \right)$$

$$\approx \frac{R_{\max}}{R_{\min}} + \left(\frac{R_{\max}}{R_{\min}} \right) \frac{\Delta R}{R_{\min}} + \frac{\Delta R}{R_{\min}} \approx \frac{R_{\max}}{R_{\min}} + 2 \frac{\Delta R}{R_{\min}}$$

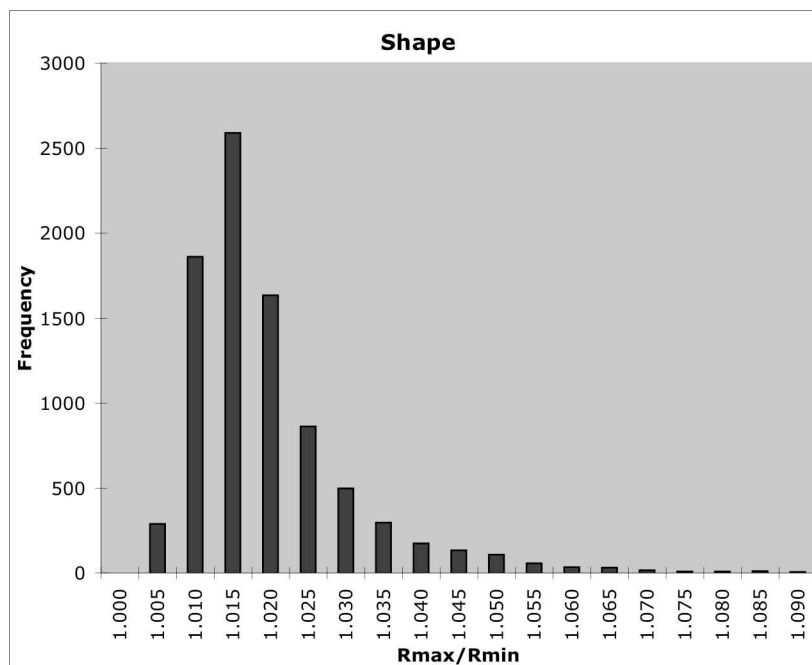
For highly aspherical particles we simply set the bias, ΔR , equal to the pixel size and calculate the offset as $2\Delta R/R_{\min}$. For more spherical particles, where the minimum uncorrected aspect ratio is near or below this offset, we use an alternate method where we estimate the offset to be equal to the minimum uncorrected aspect ratio, in order to not overestimate the offset. This is equivalent to the assumption that the most spherical particle essentially exhibits a perfect circular cross section to the limit of the measurement sensitivity. The DUN350 kernels were highly spherical, so a constant correction factor was subtracted from each sphericity (radius-based and diameter-based) so that the minimum sphericity was 1. The estimated correction factor is reported with each data set.

Image analysis of the random sample was used to calculate statistics describing the composite batch. Note that the bin values in the histograms are upper limits on each bin. The measured kernels had an average mean diameter of $355 \mu\text{m}$ with a standard deviation in the distribution of $4 \mu\text{m}$. Based on variable sampling statistics using a two-sided student's t distribution ($t=1.96$), the average mean diameter of the DUN350 composite of kernels was $354\text{--}355 \mu\text{m}$ with 95% confidence. Applying a two-sided tolerance factor test ($K=2.576$), the critical range containing 99% of the composite was $344\text{--}366 \mu\text{m}$ with 95% confidence. Applying two separate one-sided tolerance factor tests ($K=2.326$) for the upper and lower bound with a 99% tolerance limit, the critical range (with 1% above and 1% below) was $345\text{--}365 \mu\text{m}$ with 95% confidence. These values were well within the specified acceptance criteria of $350 \pm 10 \mu\text{m}$ on the mean and $<1\%$ below 300 and $<1\%$ above 400 μm . The composite passed the acceptance criteria on sphericity of $<1\%$ with $D_{\max}/D_{\min} \geq 1.05$ at 95% confidence. Applying a z-factor test (which is relevant for a sample size greater than 891) it was calculated that the minimum control limit that the composite would pass at $<1\%$ tolerance based on the measured sample was $D_{\max}/D_{\min} \geq 1.038$. Alternately, the minimum tolerance limit that the composite would pass for a control limit of $D_{\max}/D_{\min} \geq 1.05$ based on the measured sample was 0.4%.

To guide ongoing research efforts, 95% confidence intervals were determined for: (1) the sphericity limit that demarcates 1% of the composite batch and (2) the defect fraction of the composite batch (where a defect was defined as a sphericity greater than 1.05). Based on t-statistics, the 95% confidence interval for the sphericity limit that would demarcate 1% of the composite batch was 1.033-1.038. Using t-statistics, the 95% confidence interval for the defect fraction of the composite batch was 0.18-0.40%.

	Rmax/Rmin	Mean Radius	St. Dev. In Radius	Minimum Radius	Maximum Radius
Average	1.017	177	0.7	175	180
Standard Deviation	0.012	2	0.3	2	3
Minimum	1.000	159	0.3	157	161
Maximum	1.215	186	7.1	182	206

Rmax/Rmin	Frequency
1	1
1.005	289
1.01	1861
1.015	2590
1.02	1634
1.025	862
1.03	497
1.035	296
1.04	174
1.045	133
1.05	106
1.055	56
1.06	32
1.065	31
1.07	16
1.075	8
1.08	8
1.085	10
1.09	6
1.095	3
1.1	3
1.105	3
1.11	3
1.115	0
1.12	1
1.125	1
1.13	2
More	4



Mean Radius	Frequency
160	1
161	0
162	0
163	1
164	0
165	1
166	0
167	1
168	1
169	0
170	2
171	9
172	78
173	257
174	309
175	312
176	648
177	1493
178	1951
179	1810
180	1312
181	371
182	52
183	13
184	4
185	2
186	0
187	2
More	0

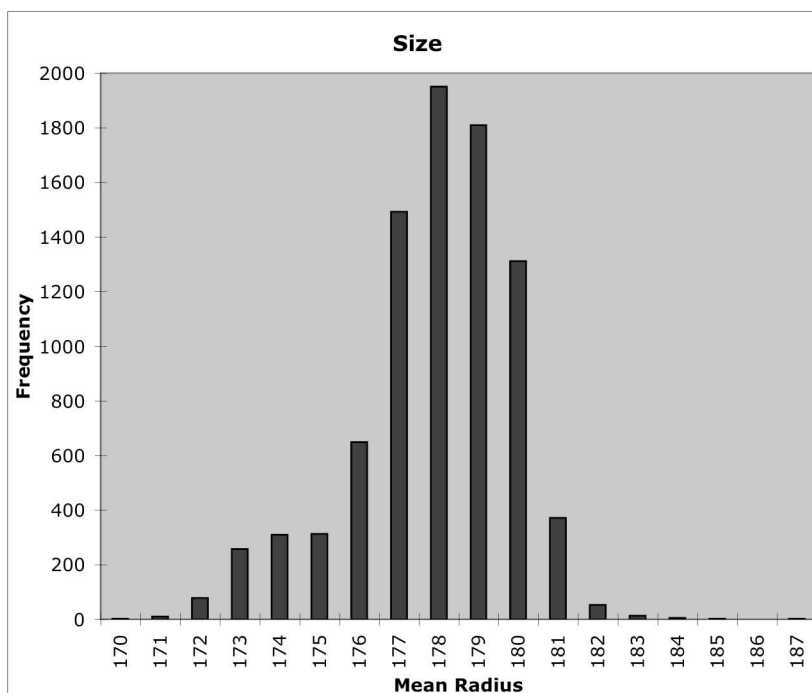
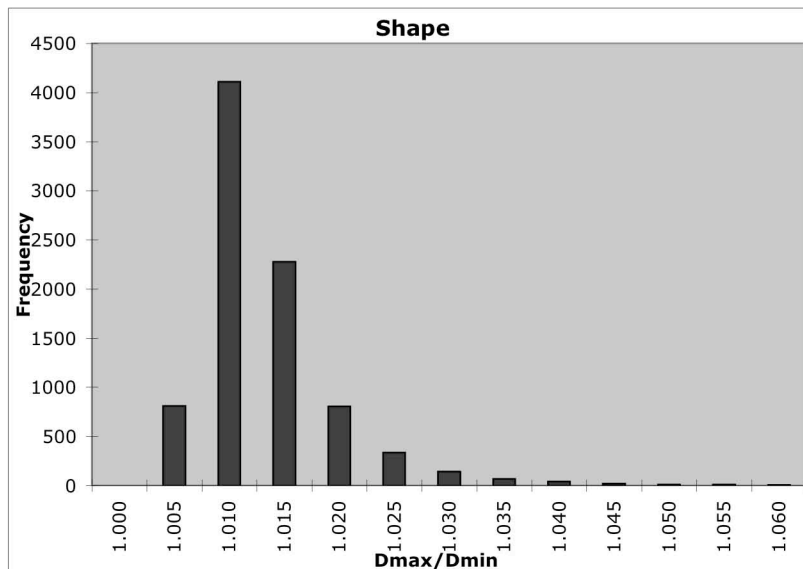


Figure 3-1: Size and shape summary for 8630 DUN350 kernels. Measurements are distance from best circle fit center to edge in μm . Measurement uncertainty is about $\pm 1 \mu\text{m}$. Estimated correction factor for sphericity offset = 0.010.

	Dmax/Dmin	Mean Diameter	St. Dev. In Diameter	Minimum Diameter	Maximum Diameter
Average	1.011	355	1.1	352	358
Standard Deviation	0.007	4	0.5	4	4
Minimum	1.000	319	0.4	317	321
Maximum	1.116	373	11.5	368	388

Dmax/Dmin	Frequency
1	1
1.005	807
1.01	4111
1.015	2277
1.02	803
1.025	334
1.03	142
1.035	66
1.04	39
1.045	16
1.05	9
1.055	9
1.06	6
1.065	2
1.07	3
1.075	2
1.08	0
1.085	0
1.09	0
1.095	0
1.1	2
1.105	0
1.11	0
More	1



Mean Diameter	Frequency
320	1
322	0
324	0
326	1
328	0
330	1
332	0
334	1
336	1
338	0
340	2
342	9
344	76
346	258
348	310
350	305
352	653
354	1486
356	1946
358	1818
360	1314
362	374
364	51
366	15
368	2
370	4
372	0
374	2
More	0

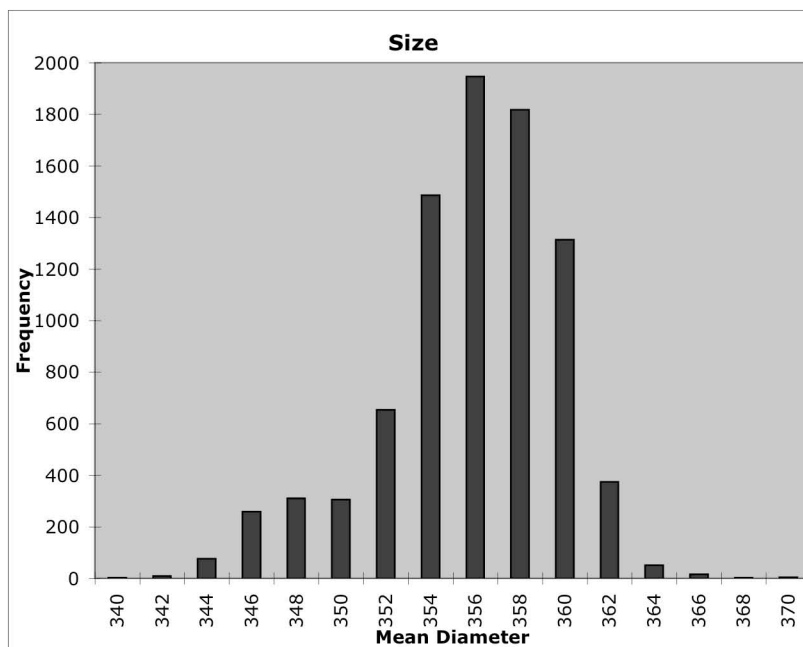


Figure 3-2: Size and shape summary for 8630 DUN350 kernels. Measurements are in μm from edge to edge through best circle fit center. Measurement uncertainty is about $\pm 1 \mu\text{m}$. Estimated correction factor for sphericity offset = 0.0053.

3.2 *Second analysis of DUN350 – higher magnification*

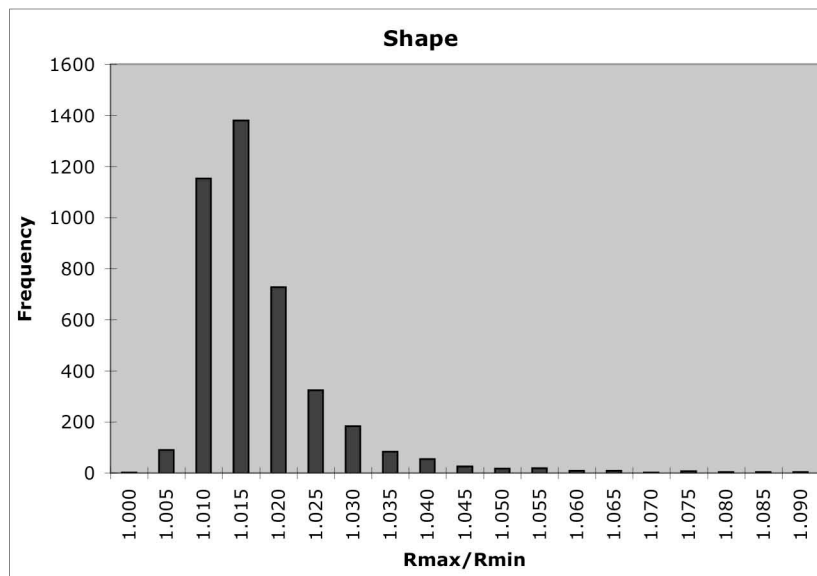
As mentioned previously in section 3.1, uncertainty in the measurement causes an offset error in the sphericity measurements. A reasonable estimate for the offset error was discussed. Since the estimated error is based on the pixel size, using a higher magnification should decrease the necessary correction factor. The problem is that the depth of focus decreases at higher magnification and this tends to offset the effect of the increased pixel resolution on the total uncertainty. A second sample of DUN350 was measured at a higher magnification ($0.442\ \mu\text{m}$ pixel size) to examine the effect of the offset error. Figure 3-3 shows the summary data for the measured radius of 4097 kernel shadowgraphs. Figure 3-4 shows the same data reported in terms of the diameter. Other than the expected reduction in the sphericity offset due to the higher resolution, the results did not differ significantly from the lower magnification measurements.

Again, the image analysis of the random sample was used to calculate statistics describing the composite batch. Note that the bin values in the histograms are upper limits on each bin. The measured kernels had an average mean diameter of $354\ \mu\text{m}$ with a standard deviation in the distribution of $4\ \mu\text{m}$. Based on variable sampling statistics using a two-sided student's t distribution ($t=1.96$), the average mean diameter of the DUN350 composite of kernels was $353\text{--}354\ \mu\text{m}$ with 95% confidence. Applying a two-sided tolerance factor test ($K=2.576$), the critical range containing 99% of the composite was $343\text{--}365\ \mu\text{m}$ with 95% confidence. Applying two separate one-sided tolerance factor tests ($K=2.326$) for the upper and lower bound with a 99% tolerance limit, the critical range (with 1% above and 1% below) was $344\text{--}364\ \mu\text{m}$ with 95% confidence. In good agreement with the low magnification results, these values were well within the specified acceptance criteria of $350\pm 10\ \mu\text{m}$ on the mean and $<1\%$ below 300 and $<1\%$ above 400 μm . The composite passed the acceptance criteria on sphericity of $<1\%$ with $D_{\text{max}}/D_{\text{min}}\geq 1.05$ at 95% confidence. Applying a z -factor test, it was calculated that the minimum control limit that the composite would pass at $<1\%$ tolerance based on the measured sample was $D_{\text{max}}/D_{\text{min}}\geq 1.035$. Alternately, the minimum tolerance limit that the composite would pass for a control limit of $D_{\text{max}}/D_{\text{min}}\geq 1.05$ based on the measured sample was 0.38%.

To guide ongoing research efforts, 95% confidence intervals were determined for: (1) the sphericity limit that demarcates 1% of the composite batch and (2) the defect fraction of the composite batch (where a defect was defined as a sphericity greater than 1.05). Based on t -statistics, the 95% confidence interval for the sphericity limit that would demarcate 1% of the composite batch was 1.029-1.036. Using t -statistics, the 95% confidence interval for the defect fraction of the composite batch was *approximately* 0.1-0.36%. This range is only approximate because the measured defect fraction was slightly too low (relative to the sample size) to declare a 95% confidence interval.

	Rmax/Rmin	Mean Radius	St. Dev. In Radius	Minimum Radius	Maximum Radius
Average	1.015	177	0.6	175	179
Standard Deviation	0.010	2	0.3	2	2
Minimum	1.000	162	0.2	160	164
Maximum	1.109	185	4.7	180	192

Rmax/Rmin	Frequency
1	1
1.005	89
1.01	1152
1.015	1380
1.02	727
1.025	324
1.03	183
1.035	83
1.04	55
1.045	26
1.05	17
1.055	18
1.06	9
1.065	9
1.07	2
1.075	7
1.08	4
1.085	3
1.09	4
1.095	1
1.1	2
1.105	0
1.11	1
More	0



Mean Radius	Frequency
163	1
164	0
165	0
166	1
167	0
168	1
169	2
170	0
171	19
172	72
173	156
174	134
175	172
176	380
177	783
178	899
179	833
180	523
181	102
182	10
183	6
184	2
185	1
More	0

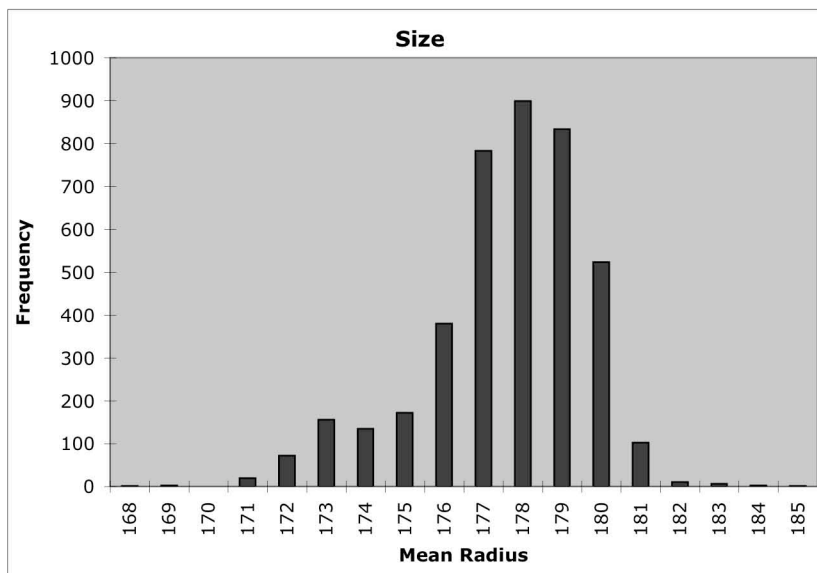
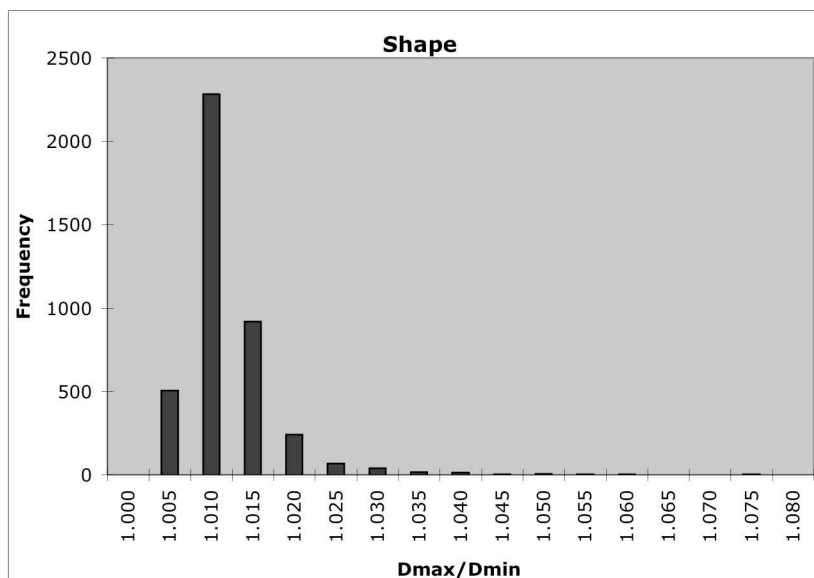


Figure 3-3: Size and shape summary for 4097 DUN350 kernels at higher magnification. Measurements are distance from best circle fit center to edge in μm . Measurement uncertainty is about $\pm 0.5 \mu\text{m}$. Estimated correction factor for sphericity offset = 0.0055.

	Dmax/Dmin	Mean Diameter	St. Dev. In Diameter	Minimum Diameter	Maximum Diameter
Average	1.009	354	0.8	352	356
Standard Deviation	0.006	4	0.4	4	4
Minimum	1.000	325	0.3	323	327
Maximum	1.080	369	6.7	363	377

Dmax/Dmin	Frequency
1	1
1.005	504
1.01	2282
1.015	919
1.02	240
1.025	67
1.03	40
1.035	16
1.04	12
1.045	3
1.05	4
1.055	3
1.06	2
1.065	0
1.07	1
1.075	2
1.08	0
1.085	1
More	0



Mean Diameter	Frequency
326	1
328	0
330	0
332	1
334	0
336	1
338	2
340	0
342	19
344	76
346	154
348	131
350	176
352	384
354	773
356	900
358	837
360	523
362	99
364	10
366	8
368	1
370	1
More	0

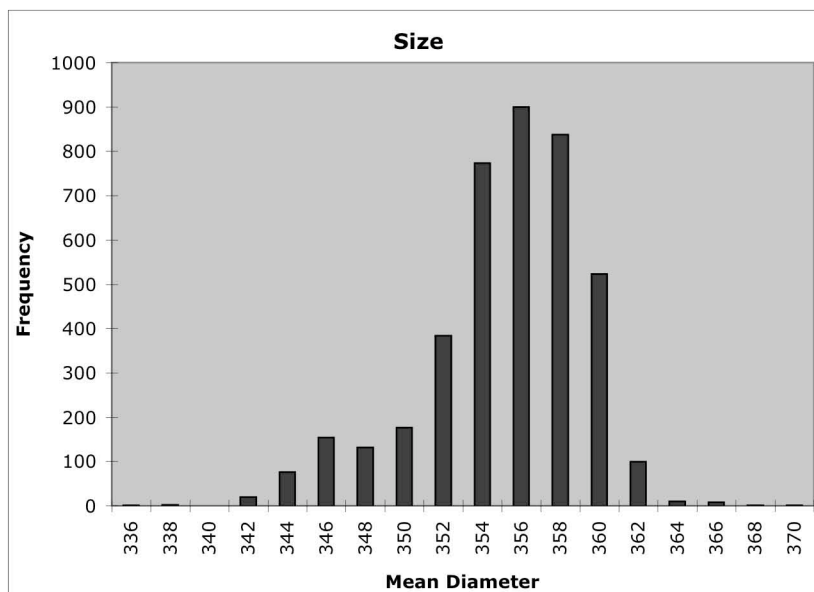


Figure 3-4: Size and shape summary for 4097 DUN350 kernels at higher magnification. Measurements are in μm from edge to edge through best circle fit center. Measurement uncertainty is about $\pm 0.5 \mu\text{m}$. Estimated correction factor for sphericity offset = 0.0029.

4 Density measurement: (Hunn, Pappano, Barker)

Using the ASTM D3766 standard terminology, we define three different types of density: the *theoretical density* is based solely on the solid material volume, the *skeletal density* includes the closed pore volume, and the *envelope density* includes the open and closed pore volume. The theoretical density of UO_2 is 10.96 g/cc.

Envelope density was measured with a Hg porosimeter. The envelope density was measured by weighing the sample and measuring the volume of mercury displaced after sufficient pressure was applied to cause the mercury to envelop each individual kernel in the sample. Open porosity information was obtained by continuing to increase the pressure and measuring the amount of mercury penetrating into the pores. Several samples were riffled from the 100 g subplot. It has been observed previously that best results with the mercury porosimeter in its present configuration are obtained for sample sizes of at least 12 g (about 50,000 kernels). Table 4-1 shows the results of the measurement of envelope density on these samples. The average envelope density was 10.92 ± 0.03 g/cc with a 0.2 ± 0.3 open porosity. The scatter in the open pore volume measurement indicates that the uncertainty in the measurement is probably greater than the measured value. However, we can conclude that the open pore volume was $<1\%$. Figure 4-1 through Figure 4-4 show the pore volume versus pore size for the four samples in the table.

Table 4-1: Envelope density by Hg porosimetry

Sample ID	Sample weight (g) ± 0.001 g	Envelope density (g/cc) ± 0.05 g/cc	% Open pore volume
DUN350-1-02	13.374	10.92	0.010
DUN350-1-05	12.357	10.87	0.580
DUN350-1-06	12.127	10.93	0.057
DUN350-1-07	11.843	10.94	0.129
Average		10.92 ± 0.03	0.2 ± 0.3

Skeletal density was measured with a helium pycnometer. The skeletal density was measured by weighing the sample and measuring the volume of helium displaced by the kernel. In this technique, the helium freely enters any open porosity in the kernels. Two samples were riffled from the 100 g subplot. The skeletal density of the samples was measured to be 10.79 g/cc and 10.81 g/cc. The average skeletal density was 10.80 ± 0.18 g/cc where the uncertainty stems mainly from the uncertainty in the calibration of the instrument. The measured skeletal density should be higher than the envelope density obtained with the mercury porosimeter, with the difference stemming from the open porosity. Given the low open porosity, these two measurements would be expected to be within 0.1 g/cc. In this case, the reported mean value of skeletal density was slightly lower. However, the expected difference between these two values was less than the reported uncertainties in the measured values, making this discrepancy insignificant.

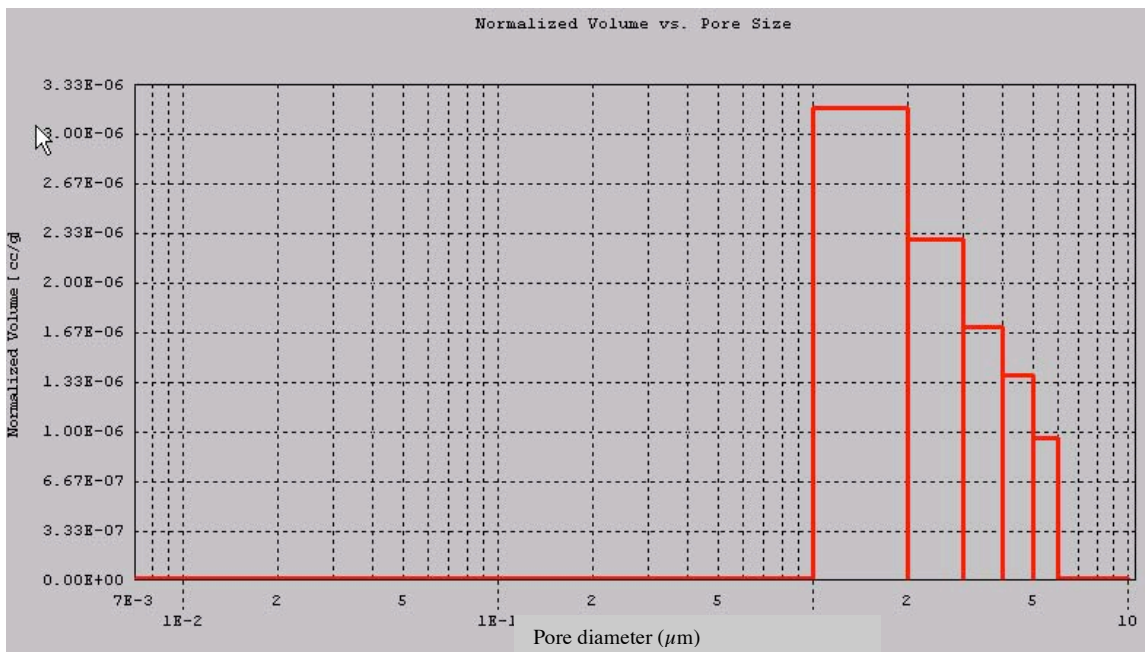


Figure 4-1: DUN350-1-02, intrusion histogram showing volume Hg per pore size.

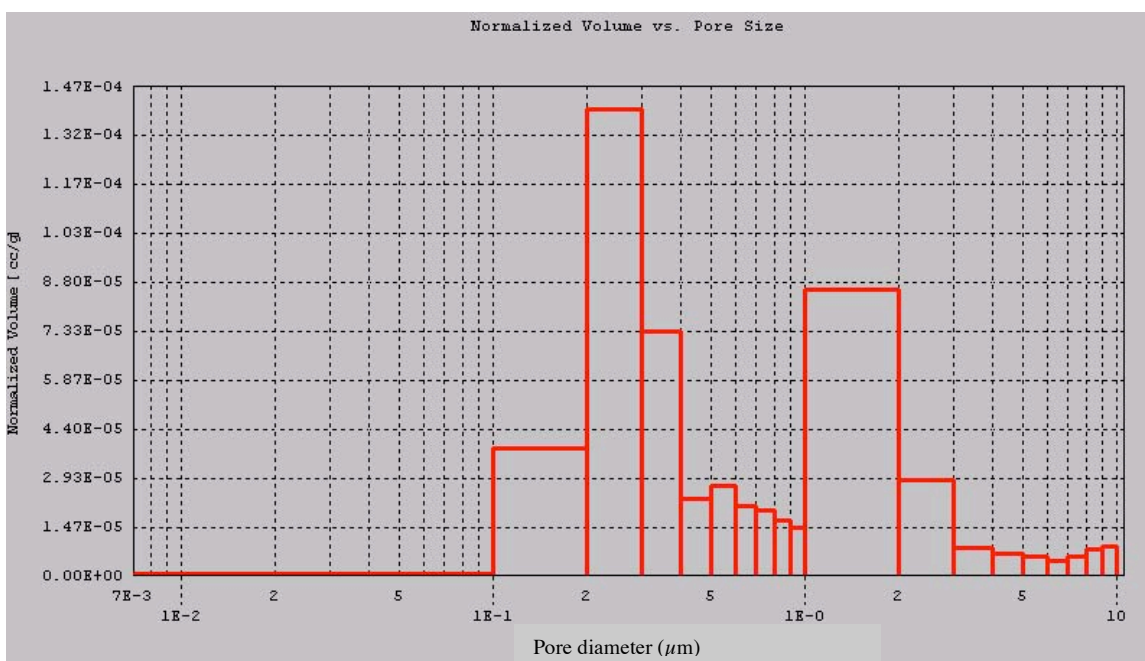


Figure 4-2: DUN350-1-05, intrusion histogram showing volume Hg per pore size.

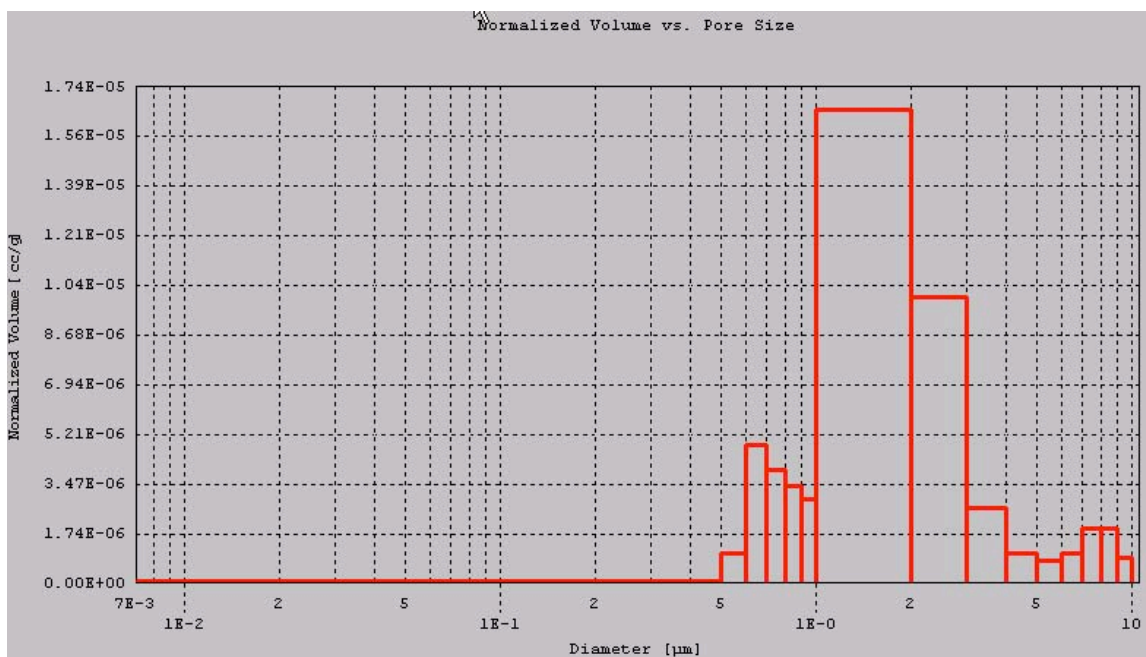


Figure 4-3: DUN350-1-06, intrusion histogram showing volume Hg per pore size.

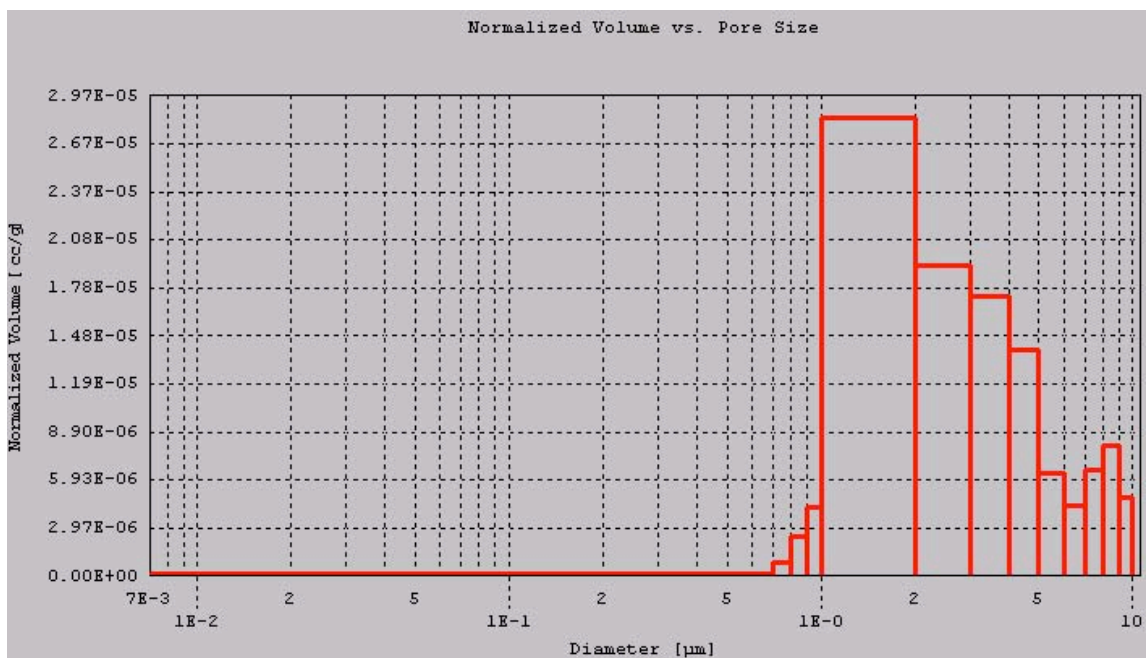


Figure 4-4: DUN350-1-07, intrusion histogram showing volume Hg per pore size.

5 Impurity analysis: (Williams, Collins, DeCul)

A 1.16 g sample of kernels (about 4700) was sent to ORNL Analytical Chemistry for analysis. The sample was microwave digested in ultra pure nitric acid to completely dissolve the sample. The uranium was then separated from the solution by using TRU resin obtained from Eichrome Technology, Inc and the collected column effluent was subsequently analyzed by ICP-MS. The only cations reported that were above the detection limit are listed in Table 5-1 (in order of decreasing concentration).

Table 5-1: Impurity analysis

Impurity Ion	Measured Concentration ($\mu\text{g/g}$ or ppm-wt)
K	15.6 ± 1.6
Cr	13.4 ± 1.3
Fe	6.31 ± 1.9
Mg	5.43 ± 0.5
Al	5.1 ± 0.5
Ni	4.5 ± 0.5
Cu	2.7 ± 0.3
Zn	2.7 ± 0.3
Mn	1.1 ± 0.2
Co	0.97 ± 0.19
Mo	0.62 ± 0.13
Sb	0.61 ± 0.12
Ba	0.38 ± 0.08
Pb	0.28 ± 0.06
Sr	0.27 ± 0.05
V	0.26 ± 0.05

ORNL delivered to Materials and Chemistry Laboratory, Inc. (MCLinc) a 4.895 g sample (about 20000) for chlorine analysis. The sample was prepared by pyrohydrolysis and analyzed by MCLinc SOP MCL-7759 Anions by Ion Chromatography. Two runs resulted in <35 and <19 chloride $\mu\text{g/g}$ (ppm-wt).

6 SEM analysis of kernel polished cross section: (Menchhofer, Hunn)

Kernels were mounted in conducting epoxy and polished to near midplane for analysis by SEM (mount ID# M040430.2). This analysis was qualitative; no attempt was made to obtain sufficient images and measurements to produce statistically sound quantitative measurements of grain size. However, it was observed that most of the polished kernels had a similar microstructure.

Figure 6-1 through Figure 6-3 show a typical kernel cross section. Imaging with back scattered electrons gave good contrast for viewing the grain structure. The grain size was less than $10\text{ }\mu\text{m}$ across in the plane of the cross section and typically about $5\text{ }\mu\text{m}$. Numerous small pits could be seen over the entire polished surface and some larger pits were also observed. The small pits, shown at high magnification in Figure 6-4, were less than $0.25\text{ }\mu\text{m}$ in diameter and appeared to be due to closed porosity exposed by the cross sectioning. Some residual scratches caused by the polishing could also be seen.

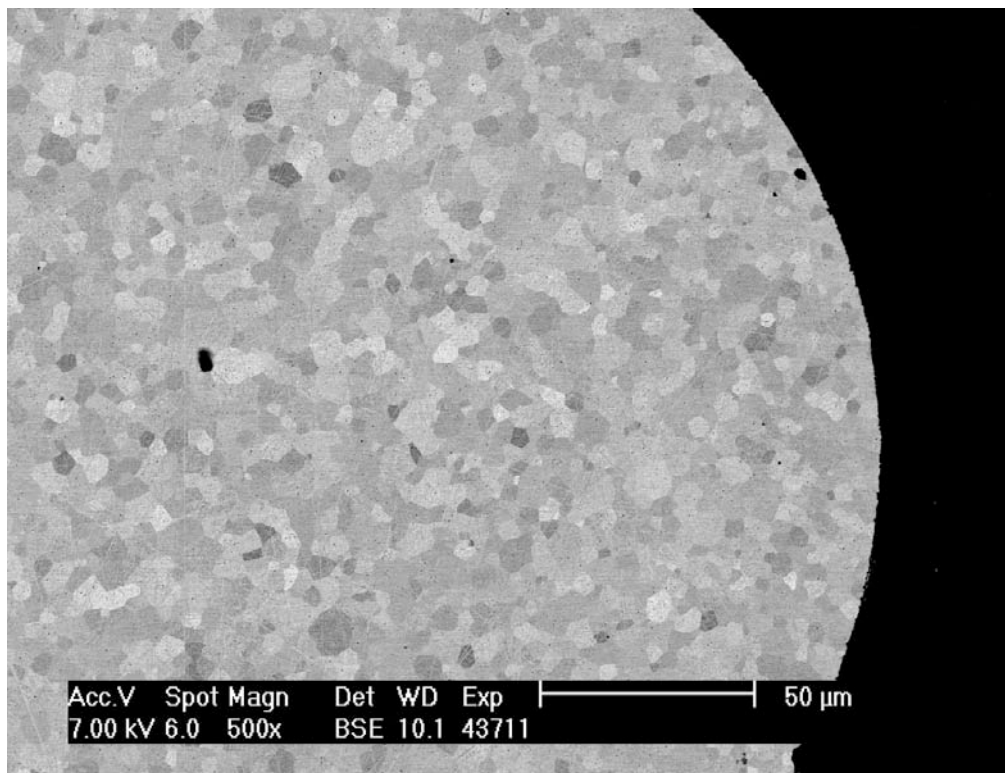


Figure 6-1: Typical cross section of DUN350 kernel.

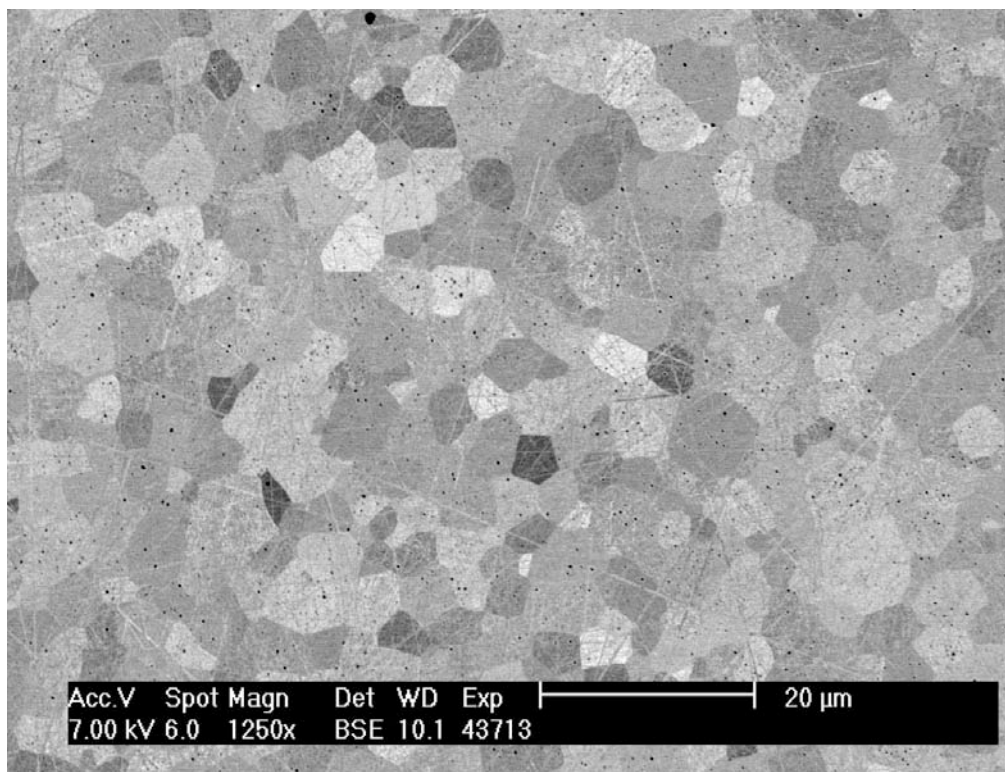


Figure 6-2: Typical cross section of DUN350 kernel.

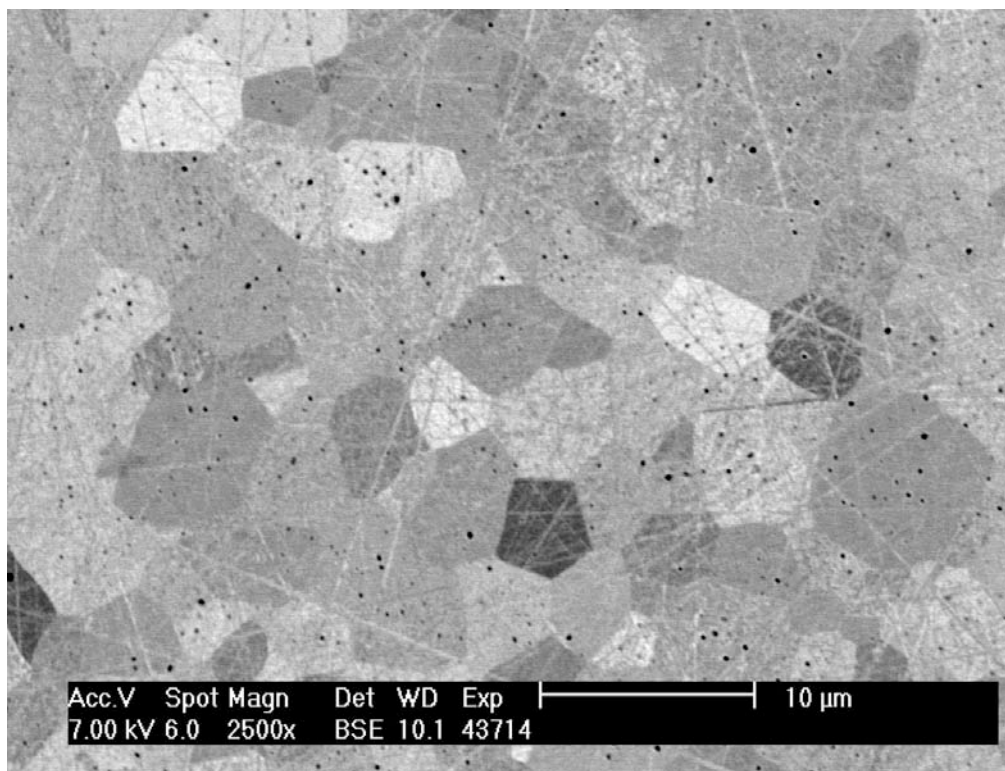


Figure 6-3: Typical cross section of DUN350 kernel.

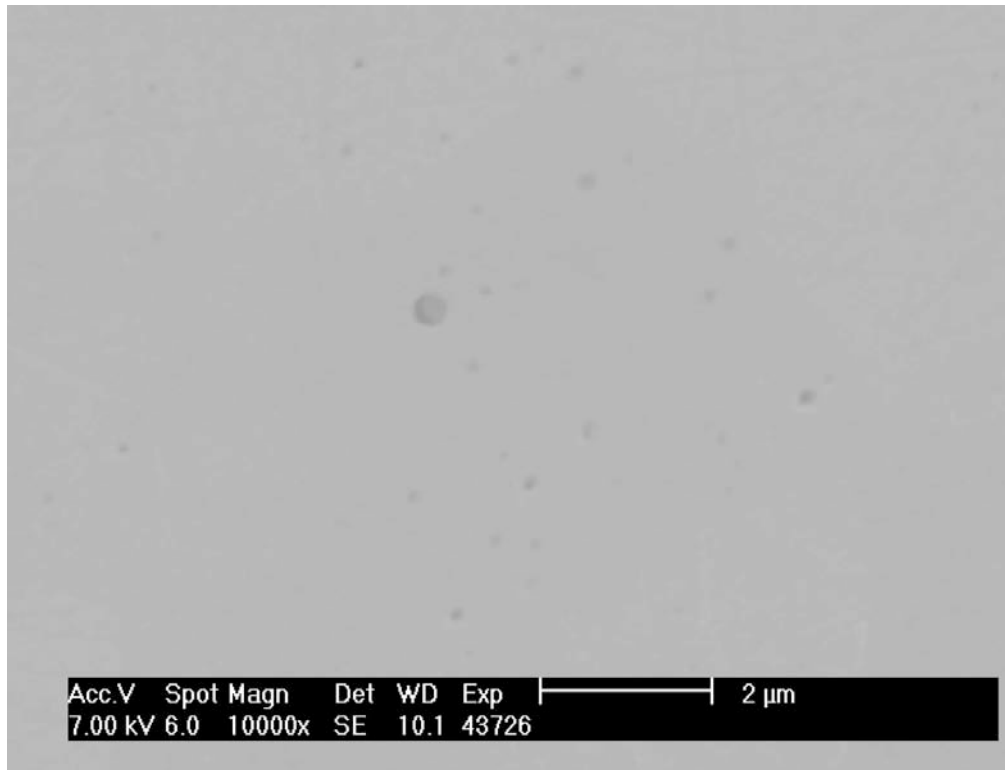
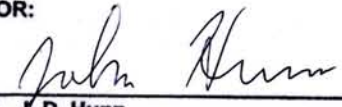
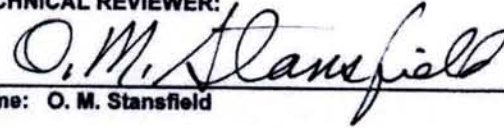
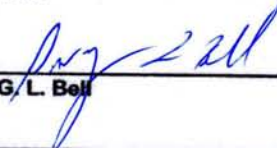


Figure 6-4: Small pits in cross section of DUN350 kernel, probably due to closed porosity.

ADVANCED GAS REACTOR PROGRAM
OAK RIDGE NATIONAL LABORATORY

ORNL DOCUMENT CLEARANCE / REGISTRATION FORM

PERSON PREPARING FORM:	PHONE NO.:	DATE SUBMITTED:
Jan Z. Palmer	576-7054	September 20, 2004
DOCUMENT NO.:	SPONSOR:	
ORNL/CF-04/12	DOE-NE / Dr. Madeline Feltus	
TITLE:		
Data Summary for Nominal 350 μ m DUO2 Kernels		
AUTHOR(s):		
J. D. Hunn		
SIGNATURES:		
AUTHOR:		
		9-23-04
Name: J. D. Hunn		Date
TECHNICAL REVIEWER:		
		9/23/04
Name: O. M. Stansfield		Date
APPROVER:		
		9/23/04
Name: G. L. Bell		Date